CSIRO PUBLISHING

Aust. J. Chem. **2016**, *69*, 458–466
http://dx.doi.org/10.1071/CH15472

Full Paper

Thermal and Spectral Analysis of Novel Amide-Tethered Polymers from Poly(allylamine)

Paolo N. Grenga,[B] *Matthew J. Nethercott,*[C] *Ayeisca E. Mateo,*[A] *Mathew Patenaude,*[D] *Todd Hoare,*[D] *David P. Weliky,*[C] *and Ronny Priefer*[A,B,E]

[A]College of Pharmacy, Western New England University, Springfield, MA 01119, USA.
[B]Department of Chemistry, Biochemistry, and Physics, Niagara University, NY 14109, USA.
[C]Department of Chemistry, Michigan State University, East Lansing, MI 48824, USA.
[D]Department of Chemical Engineering, McMaster University, Hamilton, ON L8S 4L7, Canada.
[E]Corresponding author. Email: ronny.priefer@wne.edu

Post-polymerization modification of poly(allylamine hydrochloride) was applied to synthesize a library of amide-linked polyelectrolytes with tethered aliphatic, aromatic, and cubyl moieties. The efficacy of amidation was determined to be between 12 and 98 %, depending on the electronics, sterics, and solubility of the amide linkage. ^{13}C solid-state NMR was used to further validate their structure. Thermogravimetric analysis and differential scanning calorimetry analysis indicated that none of the new polymers displayed a classic melt/freeze profile, but all displayed onset decomposition temperatures smaller than 215°C. We anticipate that the structure–property relationships observed in the resulting library of graft-modified polymers can facilitate better understanding of how to design polyelectrolytes for the construction of well-defined multilayer systems.

Manuscript received: 4 August 2015.
Manuscript accepted: 6 September 2015.
Published online: 28 September 2015.

Introduction

Since the advent of polymers in the early 1900s, numerous techniques have been developed that allow for the synthesis of linear, branched, block, or comb polymers with different fundamental structures.[1–4] Typically, polymers of all these morphologies are formed directly from monomeric precursors. However, a somewhat less utilized but still useful technique for forming polymers with different chain morphologies or compositions is post-polymerization modification.[5–7] In this approach, a polymer is first synthesized and is subsequently subjected to further chemical modifications to produce a new polymer. The benefits of this approach are that (1) polymers with chemically diverse functionalities can be prepared without being constrained to compatibility requirements with the polymerization conditions and (2) one polymer can be transformed into a large number of different polymers with significantly different properties and thus different potential applications.

Layer-by-layer assembly of polyelectrolytes is a technique that allows for facile modification of surfaces by simple charge interactions. Polyelectrolyte multilayers have been examined for use in electronically conductive polymers,[8–18] membrane filtration,[19] light-emitting diodes,[20–27] antimicrobial coatings,[28–30] anti-corrosion coatings,[31–33] and small molecule delivery vehicles[34–35] among other applications. In a typical approach, a surface is alternately introduced to two oppositely charged polymer solutions in a repetitive fashion until the desired number of layers has been obtained.[36] The polyanions and polycations used may be strong,[37] weak,[37] or pseudo (also referred to as very weak) polyelectrolytes,[38–40] although no pseudo-polycations have yet been reported. Most studies in this arena have focussed on homopolymers.[37] By applying an amidation post-polymerization modification approach using poly(allylamine hydrochloride), one of the most widely used polycations, as the backbone, we envision effectively converting this polyelectrolyte from its native polycation nature into a polyanion, a pseudo-polyelectrolyte or a polycation with lower charge density (i.e. some monomer units are capped with neutral moieties). By understanding the structure–property relationships regarding how the composition and thermal properties of this library of modified poly(allylamine hydrochloride) polymers varies as a function of the type of acid graft, we anticipate gaining insights into how to design polyelectrolyte multilayers with highly tuneable stabilities and interfacial properties according to the nature of the post-polymerization graft.

Experimental

Materials

Poly(allylamine hydrochloride) (PAH, M_w ~15000), all of the aliphatic and benzoic acids for grafting, *N*-hydroxysuccinimide (NHS), *N*,*N*′-dicyclohexylcarbodiimide (DCC), KOH, and all solvents were purchased from Sigma-Aldrich and used without

further purification. The cubane-based acids were synthesized as previously described from our laboratory.[41]

*Synthesis of PAH-H (Poly(allylamine) Free Base **1**)*[42]

PAH (2.50 g, 0.027 mol) was first dissolved in methanol (MeOH; 50 mL), after which KOH (1.56 g, 0.028 mol) was added. The resulting solution was stirred at room temperature for 15 h. The solution was then concentrated under reduced pressure (~2 mL), followed by addition of ethanol (EtOH; 50 mL) to the crude residue. An off-white precipitate formed and subjected to vacuum filtration to remove the KCl by-product. The filtrate was then concentrated to 10 mL to yield a solution of PAH-H.

*Synthesis of Amide-Tethered Polymers **2b**–**18b***[42]

The required acid (**2a**–**18a**; 1.0 molar equivalent), NHS (1.4 molar equivalent), and DCC (1.2 molar equivalent), per monomer unit, were dissolved in $CHCl_3$ and stirred at room temperature for 3 h. Different equivalents of PAH-H in EtOH were then added to the solution, after which a precipitate formed almost immediately. The mixture was stirred for an additional 3 h. The suspension was vacuum filtered, and the resulting white solid was washed with copious amounts of $CHCl_3$. The white solid was dried overnight, pulverized, triturated with copious amounts of $CHCl_3$, and left to dry overnight once more.

Elemental Analysis

Elemental analysis was conducted on a Therm FlashEA 1112 elemental analyzer. All samples were analyzed for % nitrogen, carbon, and hydrogen. Each sample was run in triplicate.

Solid-State NMR (SSNMR) Spectroscopy[43]

The samples were initially ground using a mortar and pestle to a uniform consistency for 5–10 min. A ground sample (~35 mg) was then scrapped onto a clean piece of weighing paper and funnelled into a 4 mm magic angle spinning (MAS) pencil rotor, where it was confined to the first 2/3 of the rotor.[44] Samples were stored, packed, and analyzed at room temperature. Solid-state NMR spectra were collected on a 9.4 T (400 MHz) spectrometer (Agilent Infinity Plus, Palo Alto, CA) using a 4 mm MAS triple resonance probe tuned to ^{13}C and ^{1}H nuclei at 100.8 and 400.8 MHz, respectively. Spectra were externally referenced to the methylene resonance of adamantane at 40.5 ppm,[45] and the ^{13}C transmitter was placed at 100 ppm. Sample rotation was (12000 ± 2) Hz, and spectral data were collected at room temperature. $^{13}C/^{15}N$-labelled N-acetyl leucine was used as a model compound to optimize the parameters for the ^{13}C cross-polarization ramp. The parameters included a 5 μs ^{1}H $\pi/2$ pulse (50 kHz Rabi frequency), a 1.6 ms cross-polarization contact time, a 49–69 kHz-ramped ^{13}C cross polarization, a 2 s recycle delay, 10 ms acquisition time, 2048 scans, and ^{1}H decoupling of 77 kHz. Spectral processing of the free induction decay used 100 or 200 Hz Gaussian line broadening, 5th order polynomial baseline correction, and was Fourier transformed and phased.

Thermal Measurements

Thermal properties were examined by thermogravimetric analysis (TGA; TA Instruments Q50 system) in a N_2 atmosphere and heated at a rate of 10 K min^{-1}. Differential scanning calorimetry spectra (DSC; PerkinElmer Pyris 6; N_2 atmosphere) were collected by placing the solid sample in an aluminium capsule and heating and cooling the sample at a rate of 5 K min^{-1}. All results were acquired based on multiple heating and cooling runs, thus affording the detection of the level of enthalpy change associated with each respective phase transition. The transition enthalpy, ΔH (kJ mol^{-1}), was determined from the peak area of the DSC thermogram. The transition entropy, ΔS (J mol^{-1} K^{-1}), was calculated with the equation $\Delta S = \Delta H/T$, where T was the transition temperature corresponding to the DSC maximum. The thermodynamic data reported represent the mean values of several independent measurements carried out on different samples.

Results and Discussion

We decided to focus on performing post-polymer transformation on the PAH backbone. This polymer was chosen because it is a primary amine, thus having less steric constraints. Therefore, higher coupling yields were anticipated. However, it was first necessary to convert the salt form into the 'free-base' poly (allylamine) form. [Note that PAA is the common abbreviation for poly(acrylic acid). Thus, we have abbreviated the poly (allylamine) 'free-base' as PAH-H to minimize confusion with the literature.] Menger and coworkers have reported this conversion via the use of Amberlite IRA-400 resin.[43] However, in their subsequent reactions, they employed dioxane/water as their solvent. Due to the diversity of the groups we desired to attach to the PAH-H backbone, we knew that using any aqueous media as a solvent would affect the yield. Tanaka et al.[47] and subsequently Atkinson et al.[42,48] had reported the conversion of PAH into PAH-H via simple addition of a Brønsted–Lowry base (KOH in methanol) followed by precipitation to remove the salt by-product. We attempted using this route with several other bases including diisopropylethylamine and NaH, however, we were unsuccessful. Therefore, PAH was converted into PAH-H by stirring 1 equivalent of PAH with a slight excess of KOH in MeOH for 15 h.[47] The solution was concentrated, followed by addition of EtOH and filtration to remove KCl by-product. The supernatant was concentrated to provide a solution of free PAH-H.[42] The PAH-H could then be added to an activated carboxylic acid for ultimate amidation.

As previously reported,[42,48] the use of a succinimidyl ester of the desired carboxylic acid was quite successful for tethering to amine groups. We initially focussed on using 2-acetoxybenzoic acid (more commonly known as Aspirin) as our pendant group. This was done for several reasons: (1) having a substituent on the *ortho* carbon of the aromatic ring would provide information on the steric restraints of this reaction; (2) drug-bound polymers have been reported as slow release formulations, which employ the natural secretases and proteases of the body for cleavage of the drug-polymer bond and thus release of the active agent[49,50]; and (3) the acetyl group could be selectively cleaved to form its corresponding phenol and thus a new pseudo-polyelectrolyte.[39,40]

Briefly, the desired acid NHS and DCC were stirred in $CHCl_3$ for 3 h (Scheme 1).[42] One equivalent of PAH-H in EtOH solution was then added to the stirring solution, resulting almost immediately in a precipitate; however, the solution was continually stirred for an additional 3 h to ensure complete reaction. The white solid was collected via vacuum filtration, washed, dried, pulverized, and triturated with $CHCl_3$. The solid was then left to dry overnight once more and used for future analysis. This procedure was then repeated with a variety of aliphatic, benzylic, cubyl, as well as di-carboxylic acids, affording a

library of different amide-linked PAH-based polymers (Table 1). Unfortunately, the resulting solids were insoluble in all solvents tested including H_2O, dimethyl sulfoxide, methanol, ethanol, acetonitrile, THF, acetone, chloroform, ethyl acetate, and cyclohexane; as a result, the molecular weight could not be determined via gel permeation chromatography. Samples were instead analyzed by ^{13}C solid-state NMR, elemental analysis, DSC, and TGA.

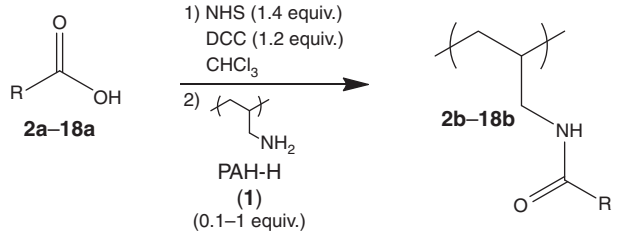

Scheme 1. Synthesis of amide-tethered polymers via amidation of PAH-H (**1**) with activated carboxylic acids **2a**–**18a**.

Our initial focus was to determine the degree to which amidation occurred as a function of the type of acid grafted. Therefore, differing ratios of the carboxylic acid to PAH-H (1 : 1, 0.5 : 1, 0.25 : 1, and 0.1 : 1) were reacted together using 2-acetoxybenzoic acid, benzylic acid, and simple acetic acid as the model acids. Elemental analysis was then used to determine the percentage conversions of the amidation reactions based on the measured % C, % H, and % N and the theoretical percentage of each element that would be present in the graft polymer at different amidation levels (Table 2).

For 2-acetoxybenzoic acid, using a 0.1 : 1 ratio of the acid to PAH-H yields 9.29 % amidation, slightly lower than the

Table 1. PAH-H (1) and carboxylic acids 2a–18a used in the synthesis of polymers 2b–18b and associated amidation percentage

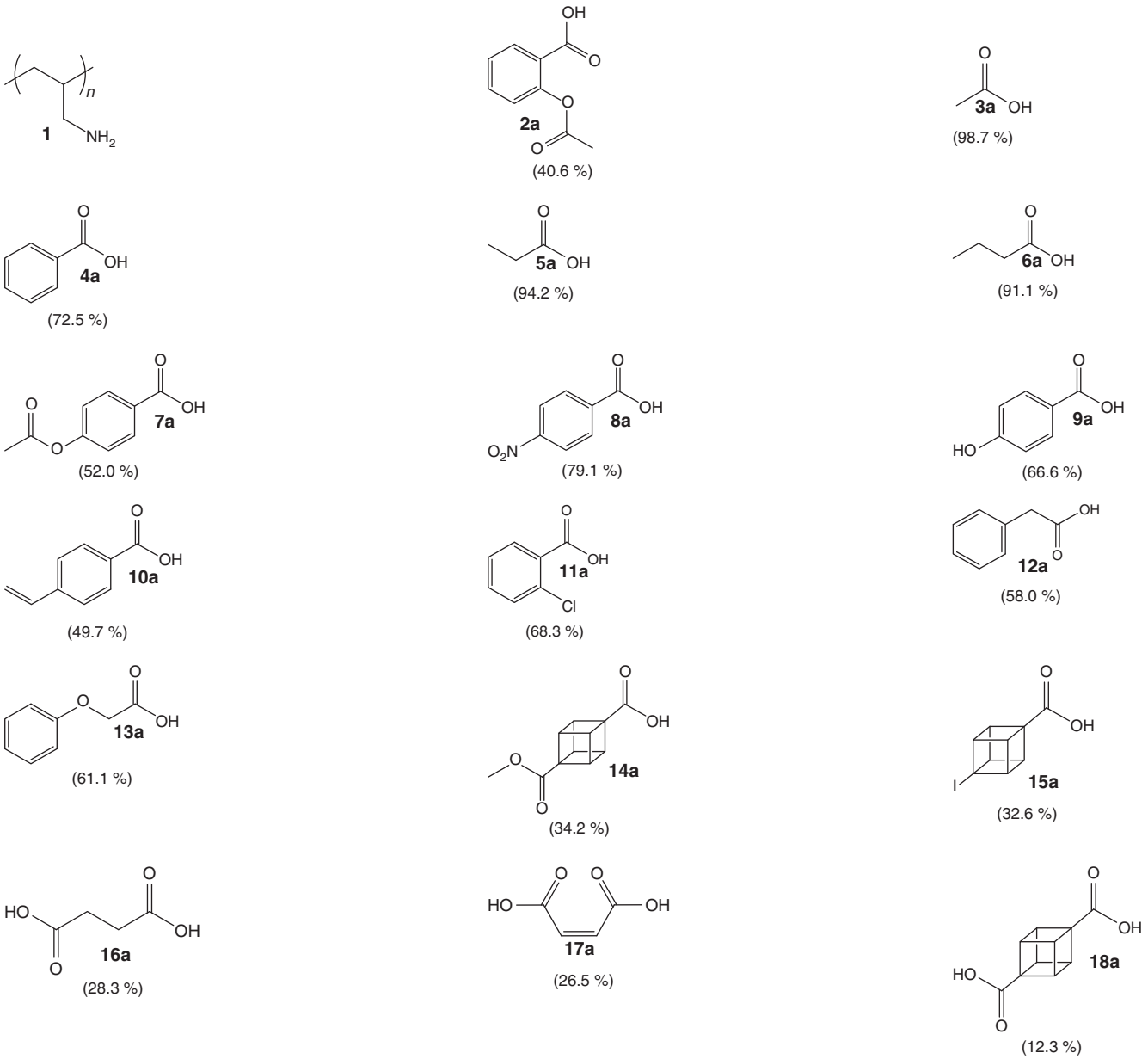

Table 2. Elemental analysis of polymer 2b and calculated percentage of amidation

Entry	Ratio (acid : PAH-H)	% C	% H	% N	% Amidation
	Elemental analysis equation	$y = 63.13 + 2.72(1 - e^{-2.994x})$	$y = 12.29 - 6.56(1 - e^{-3.030x})$	$y = 24.32 - 18.65(1 - e^{-3.030x})$	
	PAH-H (Theoretical)	(63.11)	(12.36)	(24.53)	0
1	0.1 : 1	63.77	10.65	19.78	9.29 ± 0.25
2	0.25 : 1	64.48	9.06	15.54	22.1 ± 0.90
3	0.5 : 1	65.01	7.54	11.04	40.8 ± 1.77
4	1 : 1	65.13	7.79	11.34	40.6 ± 3.25
5	0.5 : 1	65.01	7.66	11.10	40.1 ± 2.22
6	1 : 1	64.99	7.44	11.23	40.9 ± 2.94

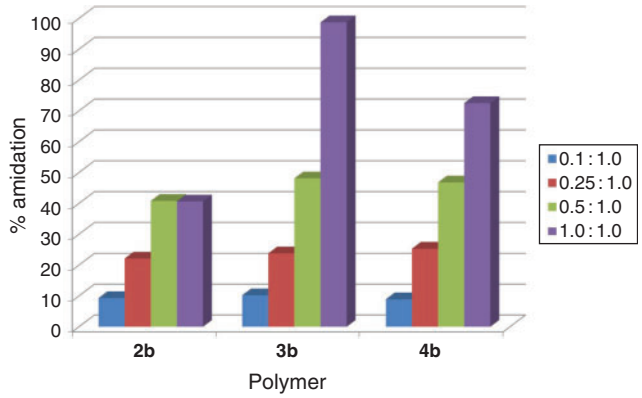

Fig. 1. Percentage of amidation of polymers **2b**, **3b**, and **4b** at different ratios of carboxylic acids (**2a**, **3a**, **4a**) to PAH-H (**1**).

theoretical 10 % (Table 2, entry 1); similarly, a 0.25 : 1 ratio leads to 22.1 % amidation (Table 2, entry 2). However, using either a 0.5 : 1 or a 1 : 1 ratio of 2-acetoxybenzoic acid to PAH-H results in a maximum of only ~41 % amidation (Table 2, entries 3 and 4). This maximum can be explained based on the observed formation of a precipitate almost instantaneously once the PAH-H was added to the preformed succinimide ester, which for all intents and purposes halted any further coupling. To confirm this result, we performed reactions using 0.5 : 1 and 1 : 1 ratios without the additional 3 h of stirring. In both cases, the % amidation was almost identical at 40.1 % and 40.9 %, respectively (Table 2, entries 5 and 6).

Using the same process as outlined above, we examined the % amidation of PAH-H with acetic acid **3a** to produce polymer **3b** and benzoic acid **4a** to produce polymer **4b** (Fig. 1). For the 0.1 : 1, 0.25 : 1, and 0.5 : 1 acid/PAH-H ratios, the % amidation achieved was largely quantitative (i.e. ~10 %, 25 %, and 50 %, respectively). However, at the 1 : 1 ratio, deviations were observed between acetic acid and benzoic acid. The use of acetic acid, **3a** (the smallest of the carboxylic acids employed in our work) led to almost complete amidation (~98 %); in comparison, the use of benzoic acid **4a** only resulted in 72.5 % coupling. Likewise, this result can be explained by the precipitation time. When PAH-H was added to the succinimide ester of benzoic acid **4b**, a precipitate formed within 10 min; in contrast, in the formation of **3b**, precipitation occurred after ~1 h of stirring. The additional time in solution allowed for a greater amount of amidation to occur and explains the near quantitative results obtained.

For the remainder of the polymers synthesized, we focussed on using 1 : 1 ratios of the carboxylic acid (**2a**–**18a**) and the PAH-H to optimize amidation (Table 1). In general, there was a decrease in the % coupling as the amount of carbon content of the carboxylic acid increased. For example, there was a drop from 98.7 % to 94.2 and subsequently 91.1 % in amidation as the carboxylic acid changed from ethanoic acid **3a** to propanoic acid **5a** and butanoic acid **6a**, respectively.

We also examined a variety of different benzoic acids (**7a**–**11a**) in addition to 2-acetoxybenzoic acid (**2a**) and simple benzoic acid **4a**. Using 4-acetoxybenzoic acid (**7a**) as opposed to 2-acetoxybenzoic acid (**2a**) resulted in an increase in coupling from 40.6 % to 52.0 %, which was attributed to a decrease in steric interactions around the carboxylate carbon. The use of 4-nitrobenzoic acid (**8a**) as opposed to 4-acetoxybenzoic acid (**7a**) resulted in a further increase in coupling from 52.0 % to 79.1 %, a result we attribute to the elevated reactivity of the starting acid (more accurately the succinimide ester) caused by the strong electron-withdrawing nature of the nitro group. In fact, acid **8a** yielded the highest coupling of any benzoic acid-based starting material. Switching to an electron-donating group in the *para* position, (i.e. a hydroxyl; **9a**) resulted in a decrease in the percentage coupling to 48.3 %, further supporting the hypothesis that the electronic nature of the substituent affects the reaction yield. Using 4-vinylbenzoic acid (**10a**) resulted in an intermediate 61.8 % coupling yield relative to **8a** and **9a**, as consistent with electronic induction effects influencing coupling yields. Finally, the use of 2-chlorobenzoic acid (**11a**), which is both electronically and sterically more favourable for coupling than 2-acetoxybenzoic acid (**2a**), resulted in a a coupling yield of 72.5 % for polymer **11b** compared with 40.6 % for polymer **2b**.

This procedure was repeated with a variety of aliphatic, cubyl, as well as mono- and di-carboxylic acids, all of which were insoluble in all solvents examined. Removal of the aromatic moiety directly adjacent to newly formed amide bond afforded polymers **12b** and **13b** with ~60 % amidation yield. However, introducing the bulkier (and slightly electron-conjugated) cubyl moiety induced a significant drop in the yield to 34.2 % and 32.6 % for the 4-methoxycarbonylcubane carboxylic acid **14a** and 4-iodocubanecarboxylic acid **15a**, respectively. Although both the ester and the iodine should electronically enhance coupling (albeit minimally), the steric bulk and the high carbon content of the cube caused ready precipitation of these novel polymers that limited conjugation yields. In parallel, when di-carboxylic acids were used, the degree of amidation for these cross-coupled polymers is further reduced to 28 % for succinic acid (**16a**), 27 % for maleic acid (**17a**), and a low of 12 % for cubane-1,4-dicarboxylic acid (**18a**).

Although all of the new polymers were insoluble in all of the solvents we employed, we wished to further examine their physico-chemical properties, particularly their thermal properties given their potential interest as ionic coatings. To that end, selected transformed polymers were subjected to TGA by

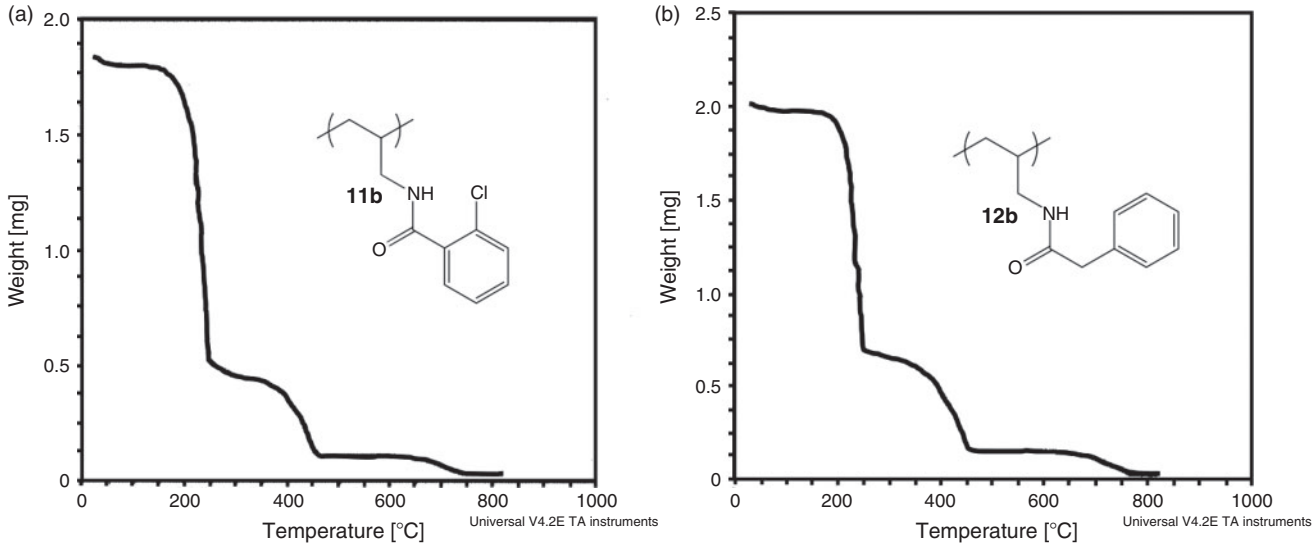

Fig. 2. Representative TGA curves of (a) **11b** (2-chlorobenozic acid/PAH-H) and (b) **12b** (phenylacetic acid/PAH-H).

placing samples in a platinum pan and exposing the samples to a temperature ramp from room temperature to 825°C. The TGA profiles obtained for polymers **11b** and **12b** (Fig. 2a, b, respectively) are representative of the profiles of all other polymers subjected to TGA. The profiles featured an initial rapid mass loss (accounting for 50–75 % of the total mass loss) followed by two less severe decreases. Regardless of the polymer, the initial onset and inflection points were ~210°C and 230°C respectively, with the exception of *p*-nitrobenzoic acid, which had an onset at 172°C and an inflection point at 208°C. Nitro-derivatized compounds are notorious for their powerful and rapid decomposition; examples of such compounds are the small molecule trinitrotoluene and the polymer nitrocellulose. The first and most significant mass loss can be attributed to thermolytic cleavage of the newly formed amide bond, whereas the second drop (accounting for loss of an additional 10–35 % of the sample mass) can be attributed to the loss of the tethered methylene amine moieties off the PAH-H backbone. Lastly, the poly (allylamine) backbone degraded to the point of near complete thermal decay at 800°C. Thus, most of the prepared polymers are thermally stable up to at least 200°C.

DSC was subsequently performed on each sample using a PerkinElmer Pyris 6 differential scanning calorimeter. Samples weighing no more than 3 mg were placed in sealed aluminium pans and subjected to heating cycles described in Table 3. This heating cycle profile allowed us to observe the endotherm melting temperature (as well as the corresponding ΔH and ΔS of that endothermic transition), the exotherm upon cooling (if present), and any thermal hysteresis that may occur (Table 3). None of the samples exhibited a DSC thermogram of a classic melting/freezing profile or a glass transition temperature. Furthermore, none of the polymers synthesized exhibited an exotherm upon cooling.

Three general types of DSC thermograms were observed. The first type of thermogram, represented by polymer **3b**, exhibited two sharp endotherms followed by a broad endotherm (Fig. 3). The double endotherms have been attributed to slow rates of heating (i.e. 5°C min^{-1} versus 20°C min^{-1}), which allow for the annealing of crystals with melting points that are lower than that of the average melting point of the material.[51] The lack of exotherm subsequently observed upon cooling is indicative of an irreversible thermal event;[52] correspondingly, the related transition temperature of the original endothermic transition matches the temperature corresponding with the initial thermolytic weight loss observed by TGA. As the DSC protocol involved a repetition of the initial temperature ramp (see Table 4), no endotherms or exotherms were observed, again indicative of sample decomposition. This was confirmed upon opening of the sample pan – a black charcoal-like substance was observed.

Polymer **4b** (Fig. 4) exhibited a DSC thermogram of the second observed type with a single, sharp endotherm at 222°C followed by a broad and less intense endotherm, which returned to the baseline heat flow by 250°C. This DSC thermogram corresponds precisely to a visual observation of this sample 'melting', as a solid sample of polymer **4b** placed in a capillary tube within a MEL-TEMP melting point apparatus began to turn from a bright white to light brown at 205°C (corresponding to the onset of the larger endotherm on the DSC thermogram) and then liquefied and condensed on the inner walls of the capillary tube at 220°C (corresponding to both the peak of the sharp endotherm on the DSC thermogram and the primary mass loss noted in TGA). At temperatures above 230°C, collapse of the solid sample was observed within the melting point apparatus, followed by browning and complete drying by 300°C. This drying and collapse of the sample correspond to the broad endotherm on the DSC thermogram, a type of endotherm previously noted as a potential indicator of decomposition of an additive to the system.[51] Visual observation of the 'melting' behaviours of polymers **8b** and **13b** also matched their respective DSC thermograms.

The final type of DSC profile was observed only with the 4-nitrobenzoic acid/PAH-H polymer **8b** (Fig. 5). In this case, only a single broad endotherm was observed at ~170°C, again matching the TGA profile. This result suggests that, unlike the other polymers, polymer **8b** does not melt but rather undergoes only a decomposition event.

Finally, the spectral profile of the novel tethered amide polymers was analyzed via ^{13}C SSNMR to confirm the functionality of the resulting polymers. The advantage of the solid-state NMR spectroscopy is that the polymer can be characterized in its natural state, without destroying or manipulating the state

Table 3. Transition temperatures, T, enthalpies, ΔH, and entropies, ΔS, for tethered amide polymers

	1st Endotherm			2nd Endotherm			Broad endotherm		
Polymer	T [K]	ΔH [kJ mol^{-1}]	ΔS [J mol^{-1} K^{-1}]	T [K]	ΔH [kJ mol^{-1}]	ΔS [J mol^{-1} K^{-1}]	T [K]	ΔH [kJ mol^{-1}]	ΔS [J mol^{-1} K^{-1}]
2b	491	23.9	16.3	–	–	–	503	69.3	46.0
3b	495	44.4	19.1	506	66.4	28.0	521	167.9	68.7
4b	489	45.8	25.8	–	–	–	499	20.8	11.5
5b	489	39.2	18.2	–	–	–	510	42.4	18.9
6b	482	22.4	11.2	–	–	–	501	51.6	24.8
7b	494	53.7	36.3	–	–	–	509	167.2	109.8
8b	–	–	–	–	–	–	447	294.8	151.6
9b	497	20.3	8.7	507	10.5	4.4	523	5.7	2.3
10b	494	60.1	36.9	506	55.9	33.5	519	161.3	94.1
11b	495	2.2	1.4	–	–	–	506	237.2	144.7
12b	495	26.7	15.6	–	–	–	503	130.4	75.0
13b	487	69.7	43.6	–	–	–	498	17.4	10.6
14b	494	51.7	37.6	506	35.3	25.1	518	113.4	78.6
15b	495	37.8	32.6	505	12.9	11.0	512	13.1	10.9
16b	493	127.5	70.1	501	12.3	6.7	517	282.4	147.9
17b	492	64.7	35.4	–	–	–	503	5.5	2.9
18b	489	265.9	187.4	–	–	–	525	27.6	19.5

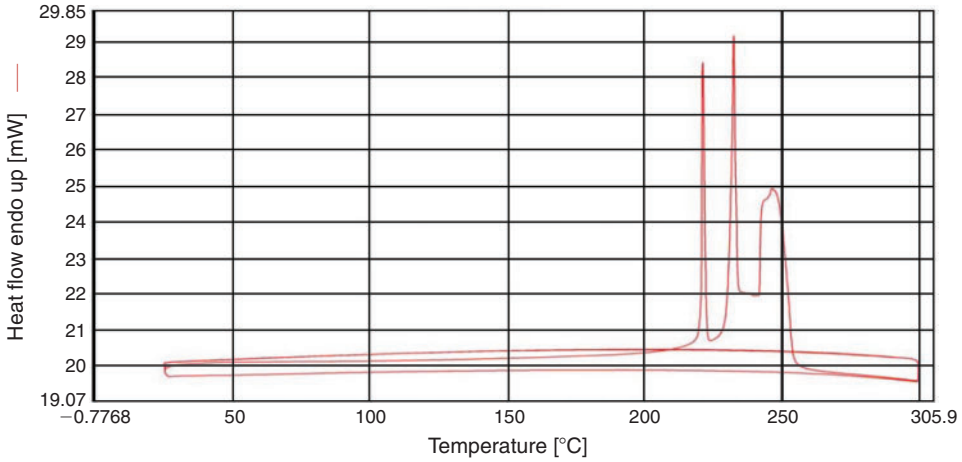

Fig. 3. DSC thermogram of acetic acid/PAH-H polymer **3b**.

Table 4. Protocol employed for the DSC analysis of polymers 12b–18b

Step	Temperature scan/isothermal
1	Hold at 30°C for 1 min
2	Heat to 300°C at 5°C min^{-1}
3	Hold at 300°C for 1 min
4	Cool from 300°C at 5°C min^{-1}
5	Hold at 30°C for 1 min
6	Heat to 300°C at 5°C min^{-1}
7	Hold at 300°C for 1 min
8	Cool from 300°C at 5°C min^{-1}
9	Hold at 30°C for 1 min

of the polymer. Using solid-state NMR spectroscopy and cross polarization, all the carbons in the system can be seen, and under suitable circumstances, the data can be quantitative. Here, the SSNMR data are only qualitative. The solid-state NMR spectra can have either broad lines or narrow lines. Any peaks corresponding to broad lines suggest that the polymers are not rigidly structured and have multiple orientations, possibly amorphous. On the other hand, sharp, narrow lines suggest that the polymer is well ordered, highly structured, and present in a limited number of orientations. The broad lines are observed for longer side chains, farther away from the polymer backbone, whereas the narrower lines would be associated with the resonances closer to a rigid polymer backbone.

Using phenylacetic acid PAH-H polymer, **12b** as an example (Fig. 6), the ^{13}C SSNMR spectrum exhibits a broad signal at ~40 ppm (corresponding to the many aliphatic carbons present in the polymer backbone), a carbonyl signal at ~180 ppm, and signals in the aromatic region (~130 ppm, indicative of the presence of the benzene ring in phenylacetic acid). [Note that a spinning side band (SSB; ~165 ppm) was also observed for many of the polymers studied.] In comparison, PAH-H (Fig. 7) only displayed signals in the aliphatic region with no signals in the aromatic or carbonyl region. For aliphatic and cubyl polymers (polymer **5b** as a representative example, Fig. 8), the carbonyl and aliphatic signals were observed, but no peaks appeared in the aromatic region (as expected).

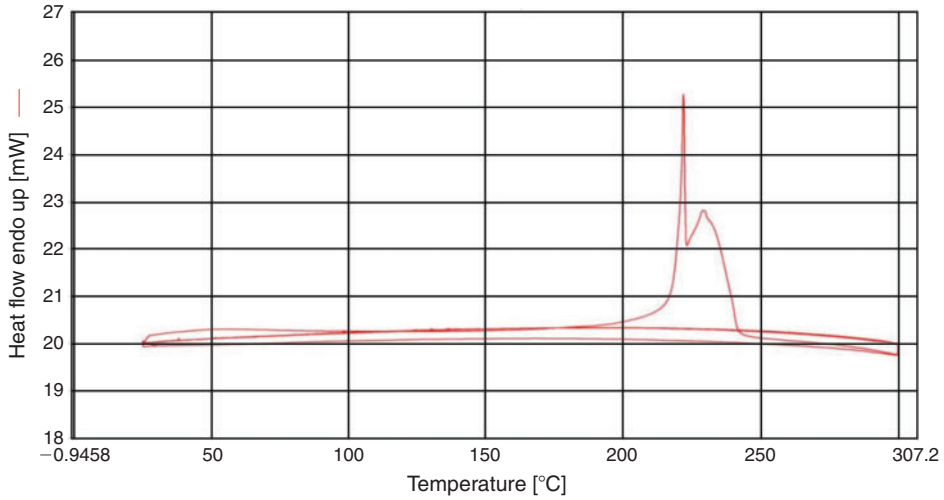

Fig. 4. DSC thermogram of benzoic acid/PAH-H polymer **4b**.

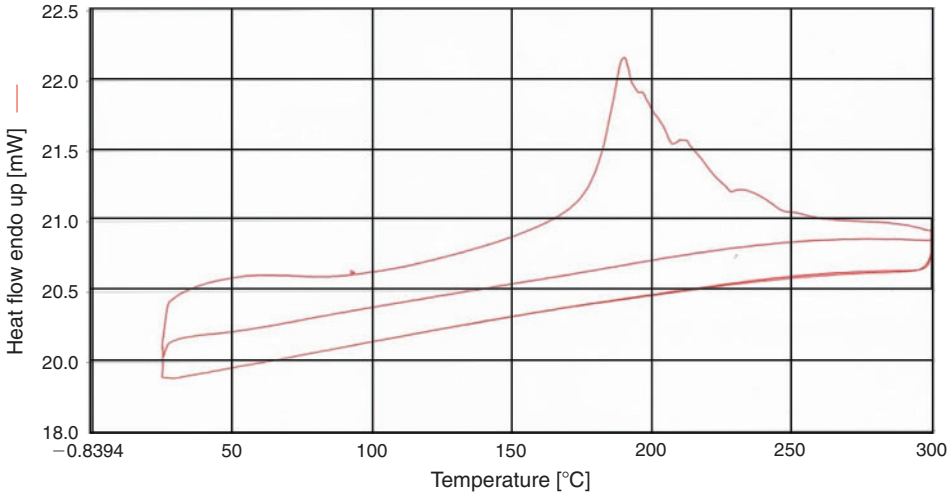

Fig. 5. DSC thermogram of 4-nitrobenzoic acid/PAH-H polymer **8b**.

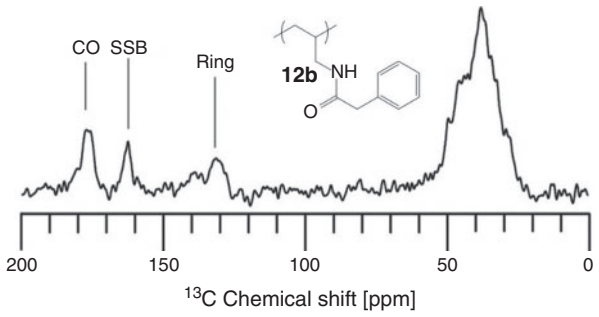

Fig. 6. Solid-state ^{13}C-NMR of phenylacetic acid/PAH-H polymer **12b**.

Conclusions

A library of polymers have been successfully synthesized by post-polymer transformation of poly(allylamine). Acid reagents with aliphatic, aromatic, and cubyl structures (including some diacids) were attached to this polymeric backbone via an amide

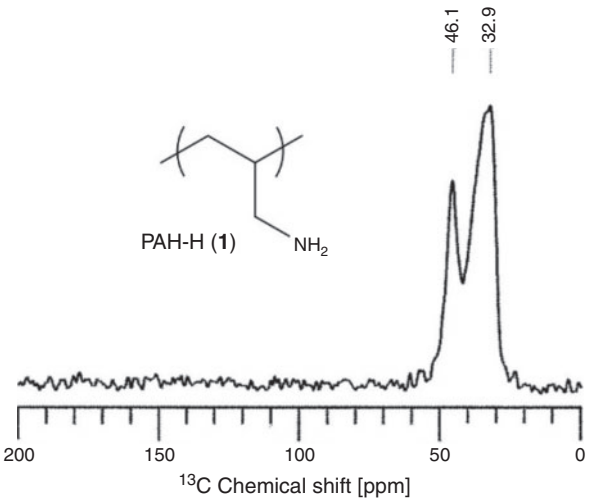

Fig. 7. Solid-state ^{13}C-NMR of PAH-H (**1**).

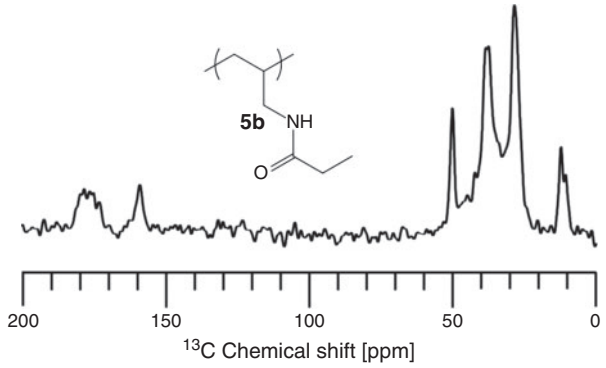

Fig. 8. Solid-state ^{13}C-NMR of propanoic acid/PAH-H polymer **5b**.

bond. Using elemental analysis, we were able to determine the degree of amidation and identify the dependence of the degree of amidation on the electronics, sterics, and degree of solubility of the acid graft. The chemical structures of these polymers were ultimately confirmed by ^{13}C SSNMR. Thermal analysis illustrated that polymers are thermally stable until heated to temperatures in excess of 200°C, with the exception of the 4-nitrobenzoic acid-grafted polymer. Differential scanning calorimetry illustrated three general means by which these polymers behave thermally, with different melting versus degradation events again related to the chemical structure. Percentages of weight loss, as indicated by TGA, provided further confidence in interpreting these thermal transitions. The structure–property relationships outlined in this work offer some insights into the practical design of soluble polyelectrolytes of various types, which may lead to well-defined polyelectrolyte multilayers.

Supplementary Material

Additional copies of DSC and NMR spectra for tethered polymers are available on the Journal's website.

Acknowledgements

We thank the American Chemical Society Petroleum Research Fund for partial support of this research. PNG and RP would like to thank the Niagara University Academic Center for Integrated Sciences as well as the Rochester Academy of Science for financial support. In addition, AEM and RP thank the Western New England University College of Pharmacy for financial support. TH and MP would like to acknowledge financial contributions from the Natural Sciences and Engineering Research Council of Canada. Solid-state NMR data were acquired at the Max T. Rogers NMR facility in Michigan State University.

References

[1] D. A. Schluter, C. Hawker, J. Sakamoto, Synthesis of Polymers: New Structures and Methods **2012** (Wiley-VCH: Weinheim).
[2] M. Leclerc, J.-F. Morin, Design and Synthesis of Conjugated Polymers **2010** (Wiley-VCH: Weinheim).
[3] Y. Chujo, Conjugated Polymer Synthesis: Methods and Reactions **2010** (Wiley-VCH: Weinheim).
[4] F. J. Davis, Polymer Chemistry **2004** (Oxford University Press: New York, NY).
[5] P. Theato, H.-A. Klok, Functional Polymers by Post-Polymerization Modification: Concepts, Guidelines, and Applications **2013** (Wiley-VCH: Weinheim).
[6] J. Romulus, J. T. Henssler, M. Weck, *Macromolecules* **2014**, *47*, 5437. doi:10.1021/MA5009918
[7] K. A. Günay, P. Theato, H.-A. Klok, *J. Polym. Sci., Part A: Polym. Chem.* **2013**, *51*, 1. doi:10.1002/POLA.26333
[8] W. B. Stockton, M. F. Rubner, *Macromolecules* **1997**, *30*, 2717. doi:10.1021/MA9700486
[9] M. Ferreira, J. H. Cheung, M. F. Rubner, *Thin Solid Films* **1994**, *244*, 806. doi:10.1016/0040-6090(94)90575-4
[10] M. Ferreira, M. F. Rubner, *Macromolecules* **1995**, *28*, 7107. doi:10.1021/MA00125A012
[11] A. C. Fou, M. F. Rubner, *Macromolecules* **1995**, *28*, 7115. doi:10.1021/MA00125A013
[12] J. H. Cheung, W. B. Stockton, M. F. Rubner, *Macromolecules* **1997**, *30*, 2712. doi:10.1021/MA970047D
[13] M. K. Ram, M. Salerno, M. Adami, P. Faraci, C. Nicolini, *Langmuir* **1999**, *15*, 1252. doi:10.1021/LA9807255
[14] J. Lukkari, M. Salomaki, A. Viinikanoja, T. Aaritalo, J. Paukkunen, N. Kocharova, J. Kankare, *J. Am. Chem. Soc.* **2001**, *123*, 6083. doi:10.1021/JA0043486
[15] G. Zotti, G. Schiavon, S. Zecchin, A. Berlin, G. Giro, *Synth. Met.* **2001**, *121*, 1381. doi:10.1016/S0379-6779(00)00981-4
[16] H. A. Kim, B. H. Sohn, W. Lee, J.-K. Lee, S. J. Choi, S. J. Kwon, *Thin Solid Films* **2002**, *419*, 173. doi:10.1016/S0040-6090(02)00779-4
[17] M.-K. Park, K. Onishi, J. Locklin, F. Caruso, R. C. Advincula, *Langmuir* **2003**, *19*, 8550. doi:10.1021/LA034827T
[18] F. Trivinho-Strixino, E. C. Pereira, S. V. Mello, O. N. Oliveria, *Langmuir* **2004**, *20*, 3740. doi:10.1021/LA035899N
[19] S. Han, B. Lindholm-Sethson, *Electrochim. Acta* **1999**, *45*, 845. doi:10.1016/S0013-4686(99)00295-9
[20] A. C. Fou, O. Onitsuka, M. Ferreira, M. F. Rubner, B. R. Hsieh, *J. Appl. Phys.* **1996**, *79*, 7501. doi:10.1063/1.362421
[21] H. Hong, D. Davidov, Y. Avany, H. Chayet, E. Z. Farggi, R. Neumann, *Adv. Mater.* **1995**, *7*, 846. doi:10.1002/ADMA.19950071006
[22] D. W. Kim, A. Blumstein, J. Kumar, *Chem. Mater.* **2001**, *13*, 243. doi:10.1021/CM000534Z
[23] M. R. Pinto, B. M. Kristal, K. S. A. Schanze, *Langmuir* **2003**, *19*, 6523. doi:10.1021/LA034324N
[24] S. Kato, *J. Am. Chem. Soc.* **2005**, *127*, 11538. doi:10.1021/JA052170N
[25] S. Kim, J. Jackiw, E. Robinson, K. S. Schanze, J. R. Reynolds, *Macromolecules* **1998**, *31*, 964. doi:10.1021/MA970781X
[26] P. K. H. Ho, M. Granstrom, R. H. Friend, N. C. Greenham, *Adv. Mater.* **1998**, *10*, 769. doi:10.1002/(SICI)1521-4095(199807)10:10<769::AID-ADMA769>3.0.CO;2-3
[27] P. K. H. Ho, J.-S. Kim, J. H. Burroughes, H. Becker, S. F. Y. Li, T. M. Brown, F. Cacialli, R. H. Friend, *Nature* **2000**, *404*, 481. doi:10.1038/35006610
[28] J. A. Lichter, K. J. Van Vliet, M. F. Rubner, *Macromolecules* **2009**, *42*, 8573. doi:10.1021/MA901356S
[29] D. Lee, R. E. Cohen, M. F. Rubner, *Langmuir* **2005**, *21*, 9651. doi:10.1021/LA0513306
[30] M. S. Pinto, M. E. McGahan, W. W. Steiner, R. Priefer, *Colloids Surf., A* **2011**, *377*, 182. doi:10.1016/J.COLSURFA.2010.12.038
[31] O. Kachurina, E. Knobbe, T. L. Metroke, J. W. Ostrander, N. A. Kotov, *Int. J. Nanotechnol.* **2004**, *1*, 347. doi:10.1504/IJNT.2004.004915
[32] D. G. Shchukin, M. Zheludkevich, K. Yasakau, S. Lamaka, M. G. S. Ferreira, H. Mohwald, *Adv. Mater.* **2006**, *18*, 1672. doi:10.1002/ADMA.200502053
[33] M. Zheludkevich, D. G. Shchukin, K. Yasakau, H. Mohwald, M. G. S. Ferreira, *Chem. Mater.* **2007**, *19*, 402. doi:10.1021/CM062066K
[34] K. Wood, J. Boedicker, D. M. Lynn, P. T. Hammond, *Langmuir* **2005**, *21*, 1603. doi:10.1021/LA0476480
[35] D. Shenoy, A. Antipov, G. B. Sukhorukov, in *Polymeric Gene Delivery* (Ed. M. M. Amiji) **2005**, Ch. 25, pp. 399–416 (CRC Press: Boca Raton, FL).
[36] G. Decher, J. D. Hong, *Makromol. Chem., Macromol. Symp.* **1991**, *46*, 321. doi:10.1002/MASY.19910460145
[37] G. Decher, J. B. Schlenoff, Multilayer Thin Films **2013** (Wiley-VCH: Weinheim).
[38] R. Priefer, K. Sowers, T. D. Krauss, M. E. McGahan, T. W. Smith, *Thin Solid Films* **2012**, *520*, 6170. doi:10.1016/J.TSF.2012.05.079

[39] R. Priefer, P. N. Grenga, A. N. Mandrino, D. M. Raymond, K. E. Leach, T. D. Krauss, *Surf. Sci.* **2010**, *604*, 59. doi:10.1016/J.SUSC.2009.10.021
[40] R. Priefer, K. E. Leach, T. D. Krauss, J. R. Drapo, M. L. Ingalsbe, M. A. van Dongen, J. C. Cadwalader, M. A. Baumler, M. S. Pinto, *Surf. Coat. Technol.* **2008**, *202*, 6109. doi:10.1016/J.SURFCOAT.2008.07.019
[41] J. R. Griffiths, G. P. Savage, R. Priefer, *Thermochim. Acta* **2010**, *499*, 15. doi:10.1016/J.TCA.2009.10.015
[42] C. E. Atkinson, *A Novel Approach to the Rational Design of Artificial Enzymes* **2001**, Ph.D. thesis, University of London.
[43] F. M. Menger, A. V. Eliseev, B. A. Migulin, *J. Org. Chem.* **1995**, *60*, 6666. doi:10.1021/JO00126A008
[44] M. J. Nethercott, *Sample Preparation and 2D Solid State Nuclear Magnetic Resonance Studies of the FP-Hairpin Construct of the HIV GP41 Protein* **2012**, Ph.D. thesis, Michigan State University.
[45] J. Yang, D. P. Weliky, *Biochemistry* **2003**, *42*, 11879. doi:10.1021/BI0348157
[46] C. R. Morcombe, K. W. Zilm, *J. Magn. Reson.* **2003**, *162*, 479. doi:10.1016/S1090-7807(03)00082-X
[47] N. Tanaka, K. Nakagawa, H. Iwasaki, K. Hosoya, K. Kimata, T. Araki, D. G. Patterson Jr, *J. Chromatogr. A* **1997**, *781*, 139. doi:10.1016/S0021-9673(97)00638-9
[48] W. B. Motherwell, C. E. Atkinson, A. E. Aliev, S. Y. F. Wong, B. H. Warrington, *Angew. Chem., Int. Ed.* **2004**, *43*, 1225. doi:10.1002/ANIE.200352370
[49] M. Mahkam, N. Sharifi-Sanjani, *Polym. Degrad. Stab.* **2003**, *80*, 199. doi:10.1016/S0141-3910(02)00388-9
[50] M. Mahkam, *Drug Delivery* **2010**, *17*, 158. doi:10.3109/10717541003604908
[51] J. Scheirs, Compositional and Failure Analysis of Polymers: A Practical Approach **2000** (Wiley: New York, NY).
[52] W.-S. Jang, A. T. Jensen, J. L. Lutkenhaus, *Macromolecules* **2010**, *43*, 9473. doi:10.1021/MA102043D